Drug Delivery Hot Paper

International Edition: DOI: 10.1002/anie.201506030
German Edition: DOI: 10.1002/ange.201506030

# Self-Assembled DNA Nanoclews for the Efficient Delivery of CRISPR–Cas9 for Genome Editing

*Wujin Sun, Wenyan Ji, Jordan M. Hall, Quanyin Hu, Chao Wang, Chase L. Beisel,* and Zhen Gu**

***Abstract:*** *CRISPR–Cas9 represents a promising platform for genome editing, yet means for its safe and efficient delivery remain to be fully realized. A novel vehicle that simultaneously delivers the Cas9 protein and single guide RNA (sgRNA) is based on DNA nanoclews, yarn-like DNA nanoparticles that are synthesized by rolling circle amplification. The biologically inspired vehicles were efficiently loaded with Cas9/sgRNA complexes and delivered the complexes to the nuclei of human cells, thus enabling targeted gene disruption while maintaining cell viability. Editing was most efficient when the DNA nanoclew sequence and the sgRNA guide sequence were partially complementary, offering a design rule for enhancing delivery. Overall, this strategy provides a versatile method that could be adapted for delivering other DNA-binding proteins or functional nucleic acids.*

The CRISPR–Cas9 platform has rapidly transitioned from an RNA-directed defense system in prokaryotes to a facile genome-editing method.[1] The editing merely requires the Cas9 nuclease and an engineered single guide RNA (sgRNA): The 20 nucleotide guide portion of the sgRNA recognizes complementary DNA sequences flanked by a protospacer adjacent motif (PAM), and Cas9 cleaves the recognized DNA.[2] The double-stranded break is then repaired through non-homologous end-joining (NHEJ) or homology-directed repair (HDR), allowing defined alterations to the targeted region.[3]

As the CRISPR–Cas9 system undergoes further development towards human therapeutics, delivery poses the major challenge. Cas9 and the sgRNA have been frequently encoded within the DNA of plasmids of viral vectors.[4] However, this DNA can randomly integrate into the genome, potentially giving rise to cancer or other genetic diseases.[5] Furthermore, the template-driven nature of gene expression limits control over the total amount of Cas9 protein and sgRNA, and off-target cleavage has been attributed to excess dosing.[6] One alternative is to use a Cas9/sgRNA ribonucleoprotein complex for delivery,[7] which enables greater control over its intracellular concentration and limits the timeframe in which editing can occur. However, delivering protein and RNA remains a central challenge in drug delivery.[8] Most protein therapeutics, such as enzymes,[9] antibodies,[10] or transcription factors,[11] suffer from low stability and poor cell-membrane permeability as a result of their fragile tertiary structures and large molecular sizes.[8] The strongly negative charges of RNA therapeutics, including siRNA or miRNA, stop them from diffusing across cell membranes, and their susceptibility to endonuclease often requires chemical modification to prevent degradation.[12] Therefore, devising an appropriate carrier to shield the protein and RNA from detrimental physiological environment and escort them simultaneously to the cell nucleus is highly desirable.

Herein, we report a novel delivery vehicle for CRISPR–Cas9 based on a biologically inspired yarn-like DNA nanoclew (NC; Figure 1). The DNA NCs were synthesized by rolling circle amplification (RCA)[13] with palindromic sequences encoded to drive the self-assembly of nanoparticles. We previously demonstrated that the DNA NCs could encapsulate the chemotherapeutic agent doxorubicin and control its release based on the environmental conditions.[14] We now hypothesized that the DNA NCs could be loaded with and deliver the Cas9 protein together with an sgRNA for genome editing. Inspired by the ability of single-stranded DNA (ssDNA) to base-pair with the guide portion of the Cas9-bound sgRNA,[15] we designed the DNA NCs to be partially complementary to the sgRNA. After loading of the DNA NCs with the Cas9/sgRNA complex, we applied a coating made of the cationic polymer polyethylenimine (PEI) to help induce endosomal escape.[16] The Cas9/sgRNA complex delivered to the cytoplasm could then be transported into the nucleus by nuclear-localization-signal peptides fused to Cas9. We expected that the resulting delivery vehicle could form uniform particles and drive the formation of targeted insertions or deletions (indels) without measurable impact on cell viability.

To demonstrate the DNA NC mediated delivery of CRISPR–Cas9, we first selected the well-characterized and

[*] W. Sun, W. Ji, Q. Hu, Dr. C. Wang, Prof. Dr. Z. Gu
Joint Department of Biomedical Engineering, University of North Carolina at Chapel Hill and North Carolina State University
Raleigh, NC 27695 (USA)
and
Division of Molecular Pharmaceutics and Center for Nanotechnology in Drug Delivery, Eshelman School of Pharmacy
University of North Carolina at Chapel Hill
Chapel Hill, NC 27599 (USA)
E-mail: zgu@email.unc.edu
Prof. Dr. Z. Gu
Department of Medicine
University of North Carolina School of Medicine
Chapel Hill, NC 27599 (USA)
J. M. Hall, Prof. Dr. C. L. Beisel
Department of Chemical and Biomolecular Engineering
North Carolina State University
Raleigh, NC 27695-7905 (USA)
E-mail: cbeisel@ncsu.edu

Supporting information for this article is available on the WWW under http://dx.doi.org/10.1002/anie.201506030.

  

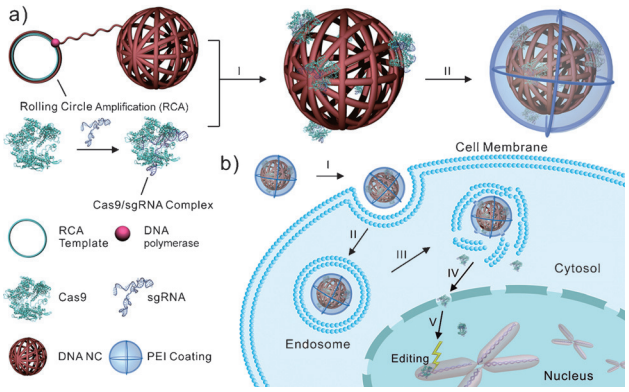


***Figure 1.*** Design of the DNA NC based CRISPR–Cas9 delivery system. a) Preparation of Cas9/sgRNA/NC/PEI. I) The NC was synthesized by RCA and loaded with the Cas9/sgRNA complex through Watson–Crick base pairing. II) PEI was coated onto Cas9/sgRNA/NC for enhanced endosome escape. b) Delivery of Cas9/sgRNA by the DNA NC based carrier to the nucleus of the cell for genome editing. I) Binding to the cell membrane; II) endocytosis; III) endosome escape; IV) transport into the nucleus; V) search for the target DNA locus in the chromosome and introduction of double-strand breaks for genome editing.

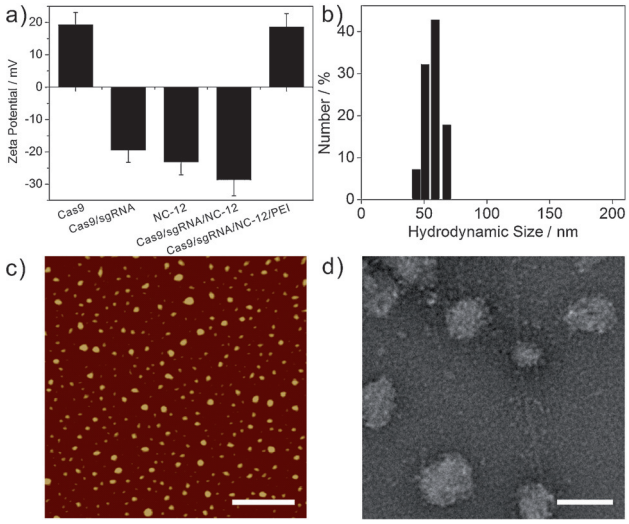


***Figure 2.*** Characterization of the Cas9/sgRNA/NC-12/PEI particles. a) Monitoring the zeta potential during the Cas9/sgRNA/NC-12/PEI assembly process. Bars represent mean ± SD ($n = 3$). b) Hydrodynamic size distribution of the Cas9/sgRNA/NC-12/PEI particles. c) AFM and d) TEM images of the Cas9/sgRNA/NC-12/PEI particles. Scale bars: 400 (c) and 100 nm (d).

extensively applied *Streptococcus pyogenes* Cas9.[17] Recombinant Cas9 fused with N-terminal and C-terminal nuclear-localization signals[18] was purified following overexpression in *Escherichia coli* (Supporting Information, Figure S1) and incubated with one of two sgRNAs: one designed to target a sequence within the enhanced green fluorescent protein (EGFP) gene flanked by an NGG PAM, and the other control sgRNA (cgRNA) designed not to appreciably target any DNA sequence in EGFP or the human genome (Figure S2a). We confirmed that the resulting Cas9/sgRNA complex was active in vitro by cleavage of a linearized plasmid encoding the *EGFP* gene, but only in the presence of Cas9 and the EGFP-targeting sgRNA (Figure S2b).

We next generated DNA NCs that bind the Cas9/sgRNA complex. The DNA template for RCA was designed to encode twelve nucleotides complementary to the 5′-end of the sgRNA (NC-12) along with the palindromic repeat that drives self-assembly (Table S1). The rationale was that the complementary sequence would promote base pairing between the DNA NC and the Cas9/sgRNA complex, thereby leading to a strong but reversible interaction. To form the nanoparticle consisting of Cas9, sgRNA, NC-12, and PEI (Cas9/sgRNA/NC-12/PEI), Cas9 and the sgRNA were incubated together, followed by the addition of NC-12 and then the addition of PEI. Measuring the zeta potential at each assembly step showed that the positively charged Cas9 ($+19.3 \pm 3.8$ mV) became negatively charged with the addition of sgRNA ($-19.4 \pm 3.7$ mV) and then NC-12 ($-28.6 \pm 5$ mV), and that the zeta potential was reverted back to a positive value upon the addition of PEI ($+18.6 \pm 4.1$ mV; Figures 2a and S3). Dynamic-light-scattering analysis (Figures 2b and S4), atomic force microscopy (Figures 2c and S4), and transmission electron microscopy (Figure 2d) revealed that the Cas9/sgRNA/NC-12/PEI nanoparticles were uniformly sized with a hydrodynamic diameter of approximately 56 nm. Interestingly, the fully assembled particle was more compact and uniformly sized than the NC-12 nanoclew and the Cas9/sgRNA/NC-12 complex, potentially because the dispersing charges are offset. To assess the co-localization of each component, we applied confocal laser scanning microscopy (CLSM) to image nanoparticles comprised of Cas9 labeled with AlexaFluor 647 (AF647), sgRNA, NC-12 stained with Hoechst 33342, and PEI conjugated with FITC. Imaging revealed consistent co-localization of all dyes (Figure S5), confirming the stable assembly of Cas9/sgRNA/NC-12/PEI nanoparticles.

We further investigated the ability of the particles to deliver Cas9/sgRNA into cultured cells. As a model, we used an established U2OS cell line that constitutively expresses a destabilized form of EGFP (U2OS.EGFP).[6b] CLSM, a technique with depth selectivity for analyzing the subcellular location of delivered drugs,[14,19] was first applied to evaluate the localization of the Cas9/sgRNA/NC-12/PEI nanoparticles containing the AF647-labeled Cas9 (Figures 3a and S6). Over the course of six hours, the labeled Cas9 first bound to the cell surface, then entered the cytosol, and was finally localized to the nuclei as indicated by the colocalization of the red fluorescence signal from AF647–Cas9 with the blue fluorescence signal of the stained nuclei. To elucidate the mechanism of internalization, we added inhibitors of different endocytosis pathways[19b] and measured the relative uptake of the Cas9/sgRNA/NC-12/PEI nanoparticles containing AF647-labeled Cas9. Flow-cytometry analysis revealed that the inhibitors methyl-β-cyclodextrin (MCD) and amiloride (AMI) imparted the greatest reduction of Cas9 uptake (Figure 3b), suggesting that the particles were mainly internalized through lipid rafts and macropinocytosis.[19b] Furthermore, we evaluated the impact of the nanoparticles on cell viability. A TO-PRO-3 live/dead assay[7a] demonstrated no

  

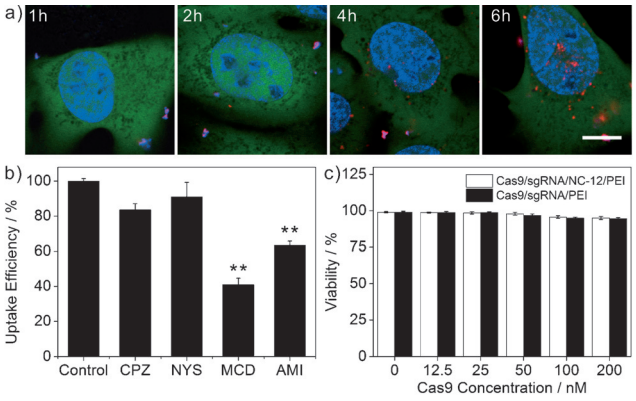


***Figure 3.*** a) CLSM images of U2OS.EGFP cells incubated with Cas9/sgRNA/NC-12/PEI for 1, 2, 4, or 6 h (Cas9 and sgRNA concentrations: 100 nM). Green: EGFP; red: Cas9 stained with AF647; blue: nuclei stained with Hoechst 33342. Scale bar: 10 μm. b) Relative Cas9/sgRNA/NC-12/PEI uptake by U2OS.EGFP cells in the presence of different endocytosis inhibitors (Cas9 and sgRNA concentrations: 100 nM). $^{**}P<0.01$ as compared to the control group. Bars represent mean ± SD ($n=3$). c) In vitro cell viability of U2OS.EGFP cells treated with Cas9/sgRNA/NC-12/PEI and Cas9/sgRNA/PEI determined by flow cytometry. The cells were subjected to a TO-PRO-3 live/dead stain after the treatment and analyzed by flow cytometry. Bars represent mean ± SD ($n=3$).

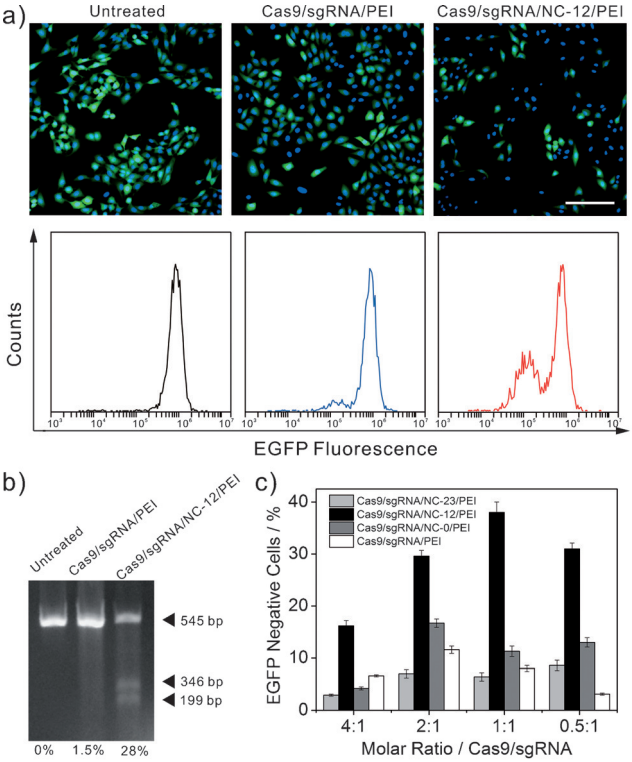


***Figure 4.*** Genome editing by Cas9/sgRNA delivered by DNA NCs (8 μg mL$^{-1}$) coated with PEI (10 μg mL$^{-1}$). a) Fluorescence microscopy images and flow-cytometry analysis of U2OS.EGFP cells treated with Cas9/sgRNA/PEI and Cas9/sgRNA/NC-12/PEI (Cas9 and sgRNA concentrations: 100 nM). Green: EGFP; blue: nuclei stained with Hoechst 33342. Scale bar: 100 μm. b) T7EI assay of U2OS.EGFP cells treated with Cas9/gRNA/NC-12/PEI and Cas9/gRNA/PEI. c) EGFP disruption assay of Cas9/gRNA delivered by different DNA NCs. The percentages of EGFP negative cells after treatment with Cas9/sgRNA/NC-23/PEI, Cas9/sgRNA/NC-12/PEI, Cas9/sgRNA/NC-0/PEI, or Cas9/sgRNA/PEI at different Cas9/sgRNA molar ratios are given. Bars represent mean ± SD ($n=3$).

measurable impact on the cell viability even at high concentrations (200 nM) of Cas9 (Figure 3c).

Based on the evidence that Cas9/sgRNA would reach the cell nucleus, we next evaluated the extent to which Cas9/sgRNA could drive the formation of indels through targeted DNA cleavage and repair by the endogenous NHEJ pathway. By targeting the coding region of EGFP, most indels would shift the reading frame, thereby preventing proper EGFP expression. To evaluate the impact on EGFP expression, we incubated cells with particles containing the EGFP-targeting sgRNA (Cas9/sgRNA/NC-12/PEI; Figure 4a) or the non-targeting cgRNA (Cas9/cgRNA/NC-12/PEI; Figure S7). Fluorescence microscopy and flow cytometry revealed that the sgRNA reduced fluorescence in approximately 36% of the cells, whereas the cgRNA had a negligible effect in comparison with the untreated cells. We also evaluated particles prepared with only Cas9, sgRNA, and PEI; these particles reduced the fluorescence in only 5% of the cells, demonstrating the importance of the DNA NCs for effective delivery. To assess whether the reduction in fluorescence could be attributed to indel formation, we applied the SURVEYOR assay, which quantifies the frequency of mutations within an amplified target region.[3] The assay revealed mutation frequencies of 28% and 1.5% for cells treated with Cas9/sgRNA/NC-12/PEI and Cas9/sgRNA/PEI (Figure 4b), respectively, closely paralleling the results of the flow cytometry analysis. We also subcloned the amplified target region of cells incubated with the Cas9/sgRNA/NC-12/PEI nanoparticles. Sanger sequencing of twenty clones revealed seven clones with typical indels within the PAM or the sequence complementary to the sgRNA guide (Figure S7), confirming the genetic disruption of EGFP expression by CRISPR–Cas9.[3] One-time treatment with the DNA NC mediated Cas9/sgRNA delivery system led to a higher editing efficacy than with the cell-penetrating peptide (CPP) based vector (9.7%) if variations of the cell line and targeted locus were not taken into account.[7b] Although the cationic lipid/anionic EGFP-based delivery strategy showed higher editing efficacy (80%),[7a] lipid vehicles often suffer from serum instability, which could be circumvented by using polymer-based carriers.[8,20]

We then asked how the complementarity between the DNA NCs and the sgRNA impacted the efficacy of Cas9-driven genome editing. To address this, we generated two additional variants of the DNA NCs with zero or 23 nucleotides complementary to the sgRNA (designated as NC-0 and NC-23, respectively). Agarose gel electrophoresis confirmed that NC-0 and NC-23 yielded similar molecular-weight distributions as NC-12 and were resistant to Cas9/sgRNA degradation (Figure S9). Subjecting the resulting particles to the U2OS.EGFP cells revealed that NC-12 yielded the highest fraction of EGFP negative cells (Figure 4c). This trend was upheld for different molar ratios of

  

Cas9 and the sgRNA, where the 1:1 standard stoichiometry of the Cas9/sgRNA complex yielded the greatest activity. Altogether, these results suggest that partial complementarity between the sgRNA and the NCs is important for efficient delivery, which may be attributed to the need for balancing Cas9/sgRNA loading and release.

We further evaluated the in vivo EGFP disruption potency of Cas9/sgRNA delivered by NC-12 using U2OS.EGFP tumor-bearing mice as models. Ten days after intratumoral injection, approximately 25% of the U2OS.EGFP cells in the frozen tumor sections near the site of injection showed no EGFP expression in the Cas9/sgRNA/NC-12/PEI treated mice, whereas the tumors in the untreated group or the group treated with Cas9/cgRNA/NC-12/PEI did not show any loss of EGFP signal (Figures 5 and S10).

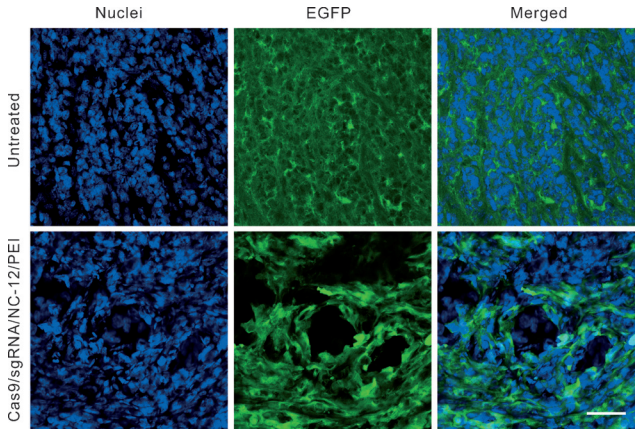


***Figure 5.*** In vivo delivery of Cas9/sgRNA into U2OS.EGFP xenograft tumors in nude mice. Tumor sections were collected ten days after intratumoral injection of Cas9/sgRNA/NC-12/PEI. The EGFPs were stained with an FITC-conjugated GFP antibody, and nuclei were stained with Hoechst 33342. Scale bar: 50 μm.

In summary, we have developed a novel delivery vehicle to achieve targeted genome editing with CRISPR–Cas9. Our DNA nanoclew based delivery system represents, to the best of our knowledge, the first example of a polymeric nanoparticle for the delivery of CRISPR–Cas9. The DNA NCs pre-organized the Cas9/sgRNA into nanoparticles and increased the charge density of the core in the core–shell assembly, which might stabilize the nanoparticle.[7a,21] Partial complementarity between the DNA nanoclew and the sgRNA guide sequence greatly enhanced the extent of gene editing, potentially because binding and release of the Cas9/sgRNA complex by the nanoclew are balanced. Future implementation of the delivery vehicles may focus on attaching cell-specific targeting ligands,[22] engineering the environmentally responsive release of CRISPR–Cas9,[14,23] modifying the sequence of the DNA NCs to incorporate multiple sgRNAs for multiplex editing, or employing the DNA NCs or packaged DNA sequences as templates for homology-directed repair. The same NC architecture could also be used to incorporate other functional DNA-binding proteins, such as transcription factors, zinc-finger nucleases, and TALE nucleases, as well as other functional or protein-coding RNAs. The potential immunogenicity associated with DNA nanoclews should be further investigated for clinical translation.[24]

## Acknowledgements

This work was supported by grants from NC TraCS, the NIH (Clinical and Translational Science Awards (CTSA, NIH grant 1L1TR001111) at UNC-CH to Z.G.), and the NSF (MCB-1452902 to C.L.B.). We thank Dr. Elizabeth Loboa and Dr. Glenn Walker for providing experimental facilities. We acknowledge Dr. J. Keith Joung from Massachusetts General Hospital for providing the U2OS.EGFP cell line. We acknowledge the use of the Analytical Instrumentation Facility (AIF) at NC State, which is supported by the State of North Carolina and the NSF.

**Keywords:** CRISPR–Cas9 · DNA · drug delivery · genome editing · nanoparticles

**How to cite:** *Angew. Chem. Int. Ed.* **2015**, *54*, 12029–12033
*Angew. Chem.* **2015**, *127*, 12197–12201

[1] P. D. Hsu, E. S. Lander, F. Zhang, *Cell* **2014**, *157*, 1262–1278.
[2] M. Jinek, K. Chylinski, I. Fonfara, M. Hauer, J. A. Doudna, E. Charpentier, *Science* **2012**, *337*, 816–821.
[3] a) L. Cong, F. A. Ran, D. Cox, S. Lin, R. Barretto, N. Habib, P. D. Hsu, X. Wu, W. Jiang, L. A. Marraffini, F. Zhang, *Science* **2013**, *339*, 819–823; b) P. Mali, L. Yang, K. M. Esvelt, J. Aach, M. Guell, J. E. DiCarlo, J. E. Norville, G. M. Church, *Science* **2013**, *339*, 823–826.
[4] a) F. A. Ran, L. Cong, W. X. Yan, D. A. Scott, J. S. Gootenberg, A. J. Kriz, B. Zetsche, O. Shalem, X. Wu, K. S. Makarova, E. V. Koonin, P. A. Sharp, F. Zhang, *Nature* **2015**, *520*, 186–191; b) R. J. Platt, S. Chen, Y. Zhou, M. J. Yim, L. Swiech, H. R. Kempton, J. E. Dahlman, O. Parnas, T. M. Eisenhaure, M. Jovanovic, D. B. Graham, S. Jhunjhunwala, M. Heidenreich, R. J. Xavier, R. Langer, D. G. Anderson, N. Hacohen, A. Regev, G. Feng, P. A. Sharp, F. Zhang, *Cell* **2014**, *159*, 440–455.
[5] M. A. Kotterman, D. V. Schaffer, *Nat. Rev. Genet.* **2014**, *15*, 445–451.
[6] a) V. Pattanayak, S. Lin, J. P. Guilinger, E. Ma, J. A. Doudna, D. R. Liu, *Nat. Biotechnol.* **2013**, *31*, 839–843; b) Y. Fu, J. A. Foden, C. Khayter, M. L. Maeder, D. Reyon, J. K. Joung, J. D. Sander, *Nat. Biotechnol.* **2013**, *31*, 822–826.
[7] a) J. A. Zuris, D. B. Thompson, Y. Shu, J. P. Guilinger, J. L. Bessen, J. H. Hu, M. L. Maeder, J. K. Joung, Z.-Y. Chen, D. R. Liu, *Nat. Biotechnol.* **2015**, *33*, 73–80; b) S. Ramakrishna, A. B. Kwaku Dad, J. Beloor, R. Gopalappa, S. K. Lee, H. Kim, *Genome Res.* DOI: 10.1101/gr.171264.113.
[8] Z. Gu, A. Biswas, M. Zhao, Y. Tang, *Chem. Soc. Rev.* **2011**, *40*, 3638–3655.
[9] T. U. Gerngross, *Nat. Biotechnol.* **2004**, *22*, 1409–1414.
[10] M. X. Sliwkowski, I. Mellman, *Science* **2013**, *341*, 1192–1198.
[11] M. Wade, Y.-C. Li, G. M. Wahl, *Nat. Rev. Cancer* **2013**, *13*, 83–96.
[12] H. Yin, R. L. Kanasty, A. A. Eltoukhy, A. J. Vegas, J. R. Dorkin, D. G. Anderson, *Nat. Rev. Genet.* **2014**, *15*, 541–555.
[13] a) M. M. Ali, F. Li, Z. Zhang, K. Zhang, D.-K. Kang, J. A. Ankrum, X. C. Le, W. Zhao, *Chem. Soc. Rev.* **2014**, *43*, 3324–3341; b) R. Hu, X. Zhang, Z. Zhao, G. Zhu, T. Chen, T. Fu, W. Tan, *Angew. Chem. Int. Ed.* **2014**, *53*, 5821–5826; *Angew. Chem.*

  

**2014**, *126*, 5931 – 5936; c) J. B. Lee, J. Hong, D. K. Bonner, Z. Poon, P. T. Hammond, *Nat. Mater.* **2012**, *11*, 316 – 322; d) H. Y. Lee, H. Jeong, I. Y. Jung, B. Jang, Y. C. Seo, H. Lee, H. Lee, *Adv. Mater.* **2015**, *27*, 3513 – 3517; e) R. J. Macfarlane, R. V. Thaner, K. A. Brown, J. Zhang, B. Lee, S. T. Nguyen, C. A. Mirkin, *Proc. Natl. Acad. Sci. USA* **2014**, *111*, 14995 – 15000; f) M. R. Jones, N. C. Seeman, C. A. Mirkin, *Science* **2015**, *347*, 1260901.

[14] W. Sun, T. Jiang, Y. Lu, M. Reiff, R. Mo, Z. Gu, *J. Am. Chem. Soc.* **2014**, *136*, 14722 – 14725.

[15] G. Gasiunas, R. Barrangou, P. Horvath, V. Siksnys, *Proc. Natl. Acad. Sci. USA* **2012**, *109*, E2579 – E2586.

[16] A. K. Varkouhi, M. Scholte, G. Storm, H. J. Haisma, *J. Controlled Release* **2011**, *151*, 220 – 228.

[17] J. A. Doudna, E. Charpentier, *Science* **2014**, *346*, 1258096.

[18] W. Fujii, K. Kawasaki, K. Sugiura, K. Naito, *Nucleic Acids Res.* **2013**, *41*, e187.

[19] a) S. Bolte, F. P. Cordelières, *J. Microsc.* **2006**, *224*, 213 – 232; b) R. Mo, T. Jiang, R. DiSanto, W. Tai, Z. Gu, *Nat. Commun.* **2014**, *5*, 3364.

[20] C. Y. M. Hsu, H. Uludag, *Nat. Protoc.* **2012**, *7*, 935 – 945.

[21] C. A. Hong, A. A. Eltoukhy, H. Lee, R. Langer, D. G. Anderson, Y. S. Nam, *Angew. Chem. Int. Ed.* **2015**, *54*, 6740 – 6744; *Angew. Chem.* **2015**, *127*, 6844 – 6848.

[22] a) D. Peer, J. M. Karp, S. Hong, O. C. Farokhzad, R. Margalit, R. Langer, *Nat. Nanotechnol.* **2007**, *2*, 751 – 760; b) E. K.-H. Chow, D. Ho, *Sci. Transl. Med.* **2013**, *5*, 216rv214.

[23] B. Zetsche, S. E. Volz, F. Zhang, *Nat. Biotechnol.* **2015**, *33*, 139 – 142.

[24] a) J. Tian, A. M. Avalos, S.-Y. Mao, B. Chen, K. Senthil, H. Wu, P. Parroche, S. Drabic, D. Golenbock, C. Sirois, J. Hua, L. L. An, L. Audoly, G. La Rosa, A. Bierhaus, P. Naworth, A. Marshak-Rothstein, M. K. Crow, K. A. Fitzgerald, E. Latz, P. A. Kiener, A. J. Coyle, *Nat. Immunol.* **2007**, *8*, 487 – 496; b) W. Sun, Z. Gu, *Biomater. Sci.* **2015**, *3*, 1018 – 1024.

Received: July 1, 2015
Revised: July 29, 2015
Published online: August 27, 2015

  